



Synthesis of mesostructured stishovite from FDU-12/carbon composite



V. Stagno^a, M. Mandal^b, W. Yang^{c,e}, C. Ji^{c,d,e}, Y. Fei^a, H.-K. Mao^{a,e}, K. Landskron^{b,*}

^a Geophysical Laboratory, Carnegie Institution of Washington, Washington, DC 20015, USA

^b Department of Chemistry, Lehigh University, Bethlehem, PA 18015, USA

^c High Pressure Synergetic Consortium, Geophysical Laboratory, Carnegie Institution of Washington, Argonne, IL 60439, USA

^d Advanced Photon Source, Argonne National Laboratory, Argonne, IL 60439, USA

^e Center for High Pressure Science and Technology Advanced Research, Shanghai 201203, P. R. China

ARTICLE INFO

Article history:

Received 23 July 2013

Received in revised form 26 November 2013

Accepted 28 December 2013

Available online 8 January 2014

Keywords:

FDU-12

Stishovite

Mesostructure

Carbon

Small-angle X-ray diffraction

ABSTRACT

Nanocasting at high pressure has been recently proposed as a novel strategy for the synthesis of periodic mesoporous materials with crystalline walls. In this study we present results on the synthesis of mesostructured stishovite from mesostructured FDU-12/carbon composite precursor using the multi-anvil press. Results from quenched experiments performed at a pressure of 14 GPa indicate that a minimum temperature of 500 °C is needed to crystallize stishovite from the amorphous silica precursor with a preserved mesostructure. Transmission electron microscopy combined with small angle X-ray scattering measurements confirmed the mesostructure of synthetic stishovite having carbon-filled pores with a diameter of ~19 nm similar to the pore size of the FDU-12 precursor. Calcination of the stishovite/carbon composite at 450 °C in air at ambient condition leads to amorphization of the stishovite. Our results show that mesostructure materials can be synthesized at very high pressures without loss or critical modification of the mesostructure.

© 2014 Elsevier Inc. All rights reserved.

1. Introduction

Periodic mesoporous materials (pore size 2–50 nm) have been considered of great interest due to their enhanced mass diffusion properties compared with microporous materials (pore of 0.5–2 nm), such as zeolites [1].

Recently, synthesis of meso-microporous zeolites with crystalline walls obtained using surfactants has been shown to have more efficient catalytic properties for various organic reactions than conventional zeolites or amorphous mesoporous molecular sieves [2,3]. More recently, we described a successful synthesis route to obtain mesoporous quartz and its high pressure polymorph coesite by a novel nanocasting route at high pressure starting from periodic mesostructured precursors, such as SBA-16 and FDU-12 [4,5] having pores initially filled with amorphous carbon. In these materials the crystalline pore walls are non-zeolitic.

Synthesis of periodic mesostructured high-pressure silica polymorphs are of particular interest as they combine physical properties such as hardness and luminescence that can potentially broaden the industrial use of these materials [6–8]. This is the case for high-pressure silica polymorphs such as coesite and stishovite that have been shown to possess high photo-luminescence induced by irradiation [9]. In particular, stishovite is a high-pressure polymorph of quartz and one of the hardest materials, with a

hardness of 33 GPa, high density (~4.35 g cm⁻³) and refractive index (~1.8). Further, stishovite like diamond is known to possess low cytotoxicity so that can be injected into the human body in extremely small amounts for light-induced medical applications, such as vehicle for drug delivery into cells in cancer therapy [10].

Here we present our results regarding the behavior of FDU-12/carbon composite at extreme conditions (14 GPa) using a multi-anvil apparatus at temperatures between 100–500 °C to test the feasibility for synthesis of mesoporous/mesostructured stishovite at high pressure and temperature. Previously, similar experiments at high pressure were performed using mesostructured silica/carbon composite starting material and resulted in loss of initial periodic mesostructure of the precursor with crystallization of nanoparticles or phase separation between crystalline stishovite and graphite [11,12].

A possible procedure for carbon removal is also described that accounts for the low amorphization temperature of stishovite and possible effects on the stability of the mesopores.

2. Materials and methods

Experiments were performed using periodic mesoporous silica FDU-12/carbon composite (*fcc* symmetry) as a starting material. The spherical mesopores with pore size of ~19 nm were completely filled with carbon resulting in negligible surface area for the composite material. Details about the synthesis procedure were described by Mohanty et al. [4]. We performed experiments

* Corresponding author. Fax: +1 610 758 6536.

E-mail address: kal205@lehigh.edu (K. Landskron).

at 14 GPa in a 1500-ton Kawai-type press available at Geophysical Laboratory (Carnegie Institution of Washington). Tungsten carbide anvils of 8 mm truncation edge length (TEL) were used with Cr₂O₃-doped octahedra (14 mm edge length) as pressure media. A cylindrical rhenium capsule (2 mm diameter by 3 mm height) was placed in the central portion of a cylindrical straight rhenium furnace, surrounded by an MgO sleeve and spacers. No ZrO₂ thermal insulator was needed because of the relatively low temperature used for the purpose of this study (≤ 500 °C). Pressure calibration of the employed assembly was performed using the phase transitions of quartz to coesite, CaGeO₃ garnet to perovskite, coesite to stishovite and olivine to wadsleyite [13]. The temperature during the experiments was monitored with a W-5%Re/W-26%Re (C type) thermocouple inserted within an alumina sleeve, with the junction in contact with the top of the capsule. The sample was compressed to the target pressure at a rate of 2 GPa/h, then heated to a temperature of 100–500 °C and kept manually constant within ± 5 °C for periods of 1–3 h. The experiments were, then, quenched by turning off the power to the furnace and decompressed at a rate of 0.5 GPa/h. Recovered samples were mounted on a stub using adhesive carbon tape for textural observation by Field Emission Scanning Electron Microscope (JEOL JSM 6500F), while phase identification was performed by powder X-ray diffraction (XRD) using both a Bruker 2D-Phaser diffractometer (Cu K α radiation) and a Rigaku R-Axis Rapid-S diffractometer (Mo K α radiation) operating at 40 kV and 30 mA with area detector, and with samples mounted on the tip of a 0.5 mm diameter glass capillary. Each phase was then indexed using Jade 6.0 software and relative PDF data files used as reference patterns.

Small angle X-ray scattering (SAXS) data were collected at ambient conditions to characterize the mesoscale periodicity of the materials. Measurements were performed at beamline 12ID-B at the Advanced Photon Source (APS), Argonne National Laboratory. A 2 M Pilatus Area detector placed at a distance of 2 m from the sample was used to record the SAXS intensity. A monochromatic wavelength of 1.033 Å was used. The displayed Intensity vs. Q profile was subtracted from background at empty area. As this is a technique sensitive to the relative density variation, the difference in density of the SiO₂ phases (stishovite, coesite, and amorphous) to either carbon or air is large enough to show strong SAXS signal.

Textural characterization at the nanoscale and analyses of the silica material quenched at high pressure was performed by JEOL JEM-2000 transmission electron microscopy (TEM) operated at an accelerating voltage of 200 kV. In this case, sample particles were dispersed in acetone and deposited on a Cu grid coated with amorphous carbon foil. Several particles were investigated for each sample in order to verify its homogeneity. N₂ sorption measurements were performed using a Quantachrome Autosorb-1 instrument with an average of 7–10 mg of sample powder. Finally, SPI Plasma-Prep II plasma etcher was employed to remove the carbon template in about 5–15 h from the recovered high-pressure silica polymorph.

3. Results and discussion

X-ray diffraction (XRD) data were collected from the recovered samples at the aim to constrain the conditions for the synthesis of mesostructured high pressure silica polymorphs. Fig. 1 shows the typical diffraction pattern of stishovite for the sample quenched at 14 GPa and 500 °C. The sharp and well resolved diffraction peaks can be unambiguously attributed to P4₂/mnm tetragonal crystal structure (JCPDS file 45-1374) with refined lattice parameters $a = 0.4196(6)$ nm and $c = 0.2667(5)$ nm comparable to the standard values of $a = 0.4179$ nm and $c = 0.2665$ nm. The broad peak at

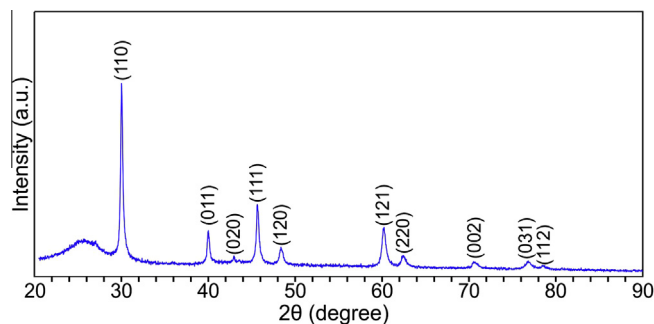


Fig. 1. X-ray diffraction pattern (Cu K α radiation) of recovered stishovite after 3 h at 14 GPa and 500 °C.

$2\theta \approx 25^\circ$ confirms the presence of carbon filling the initial mesopores in as-synthesized FDU-12. However, no transformation was observed for the carbon phase under the considered P-T conditions.

Microscopic observations of the recovered stishovite performed using the FE-SEM showed no evidence for the presence of single nanocrystals (Fig. 2a). In contrast, images obtained with secondary electrons revealed a dotted texture likely due to the weak contrast between the stishovite crystalline frame and the pores filled with carbon. Textural features of the synthetic samples were also accurately investigated by TEM. Images were collected from the quenched sample and surprisingly showed the presence of mesostructured stishovite with carbon filled mesopores homogeneous in size (Fig. 2b). Although the sample was confirmed to be crystalline using XRD measurements, however, Fig. 2b shows no diffraction spots in the reciprocal space (SAED inset) likely due to amorphization of stishovite induced by electron beam irradiation [14]. Energy-dispersive X-ray (EDX) measurements excluded possible contamination of the synthetic material by showing only peaks relative to the starting composition.

In order to prevent amorphization of stishovite by thermal treatment [15,16] and minimize the temperature effect on the mesostructure, wet chemical oxidation and subsequent oxygen plasma etching were adopted as possible techniques for removing the carbon from the pores. These techniques allowed us to test the possibility to obtain mesoporous stishovite from mesostructured stishovite by removing all the carbon from the pores. In the first case the sample powder was heated at 100–150 °C for 24 h in HClO₄ in absence of metallic catalysts to avoid contamination. A TEM image of the stishovite sample after treatment with acid is shown in Fig. S1 (Supplemental Informations). Although most of the carbon is still preserved within the pores, the SAED pattern (inset) shows evidence for the crystalline walls.

In addition, the recovered stishovite sample was also treated using oxygen plasma for carbon removal during which a maximum temperature of 50 °C is commonly achieved. After 15 h of treatment the sample powder presented a black tending to grey color. Images collected using TEM for this sample are shown in Fig. 3a and b where the mesostructure of synthetic stishovite can be clearly observed at the nanoscale along with the retained crystalline walls confirmed by the reflections in SAED pattern to be stishovite (inset in Fig. 3a). We investigated several particles to make sure that sample inhomogeneity is unlikely an issue. For this sample we were able to index the electron diffraction pattern, which is in accordance with the structure of stishovite. Based on TEM images a pore size of ~ 16 – 18 nm could be directly measured, which is in agreement with the initial pore size of calcined FDU-12 (~ 19 nm). This similarity in the pore size was also reported in a previous study [4] and can be considered as evidence that the carbon template prevents collapse of pores as a consequence of the volume change and densification due to crystallization of the

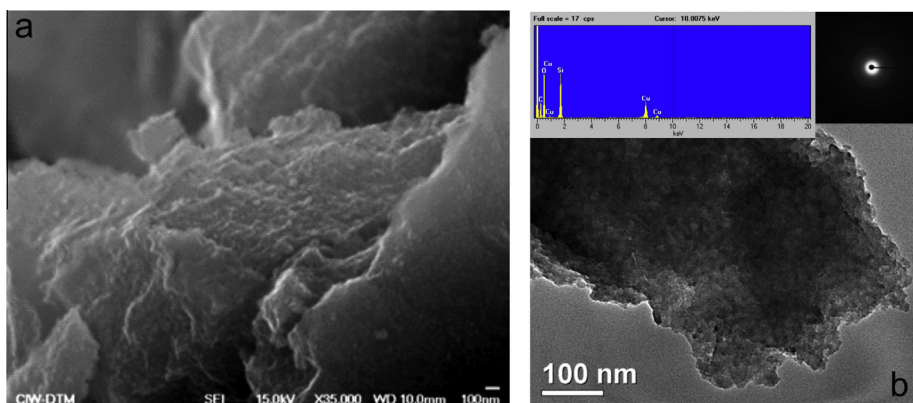


Fig. 2. (a) SEM and (b) TEM image of the recovered stishovite after 3 h at 14 GPa and 500 °C. SAED (inset) and EDX spectrum.

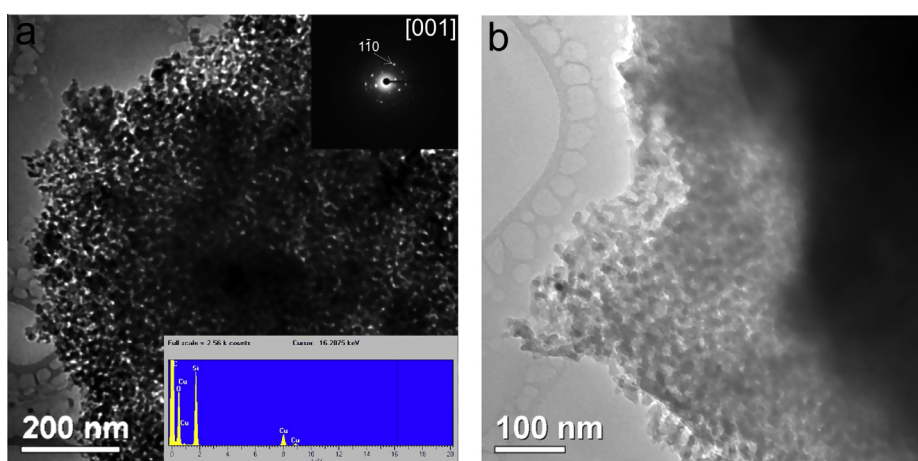


Fig. 3. (a, b) TEM image of mesostructured stishovite recovered from 14 GPa and 500 °C after plasma etching treatment with relative SAED and EDX spectrum (inset).

high-pressure phase, stishovite, during the high pressure and temperature of synthesis.

N₂ sorption measurements of these treated stishovite samples were performed at –196 °C and repeated to confirm the reproducibility of the obtained results. Measurements on both stishovites after acid attack and oxygen plasma etching showed very little adsorption at p/p_0 below 0.1 (see [Supplemental Informations](#)). The absence of a type IV isotherm can be likely explained by incomplete removal of the carbon from the pores. This may be because of insufficient reactivity of the etchants and/or the presence of closed (non-interconnected) pores as consequence of the crystallization of stishovite which traps carbon in the pores.

Small angle X-ray scattering (SAXS) is very sensitive to the particle and pore size distribution at the nanoscale, which is a non-destructive characterization technique to characterize a mesostructure without altering the quenched sample. We applied the SAXS technique on the quenched mesostructured stishovite etched sample. The intensity vs. Q value in log/log scale shows a distinguished peak at Q around 0.033 \AA^{-1} followed by a broad bump centered at around 0.06 \AA^{-1} (Fig. 4). The peak at 0.033 \AA^{-1} indicates a pore size around 19 nm, while the broad bump is due to higher order scattering. The broad feature indicates the degree of periodicity is low. The intensity of the scattering is low which is most likely due to the low electronic contrast associated with the presence of carbon within the pores.

Several experiments were performed at 14 GPa for 3 h to determine the lowest temperature needed to synthesize mesostructured stishovite from FDU-12/carbon composite. Results are summarized

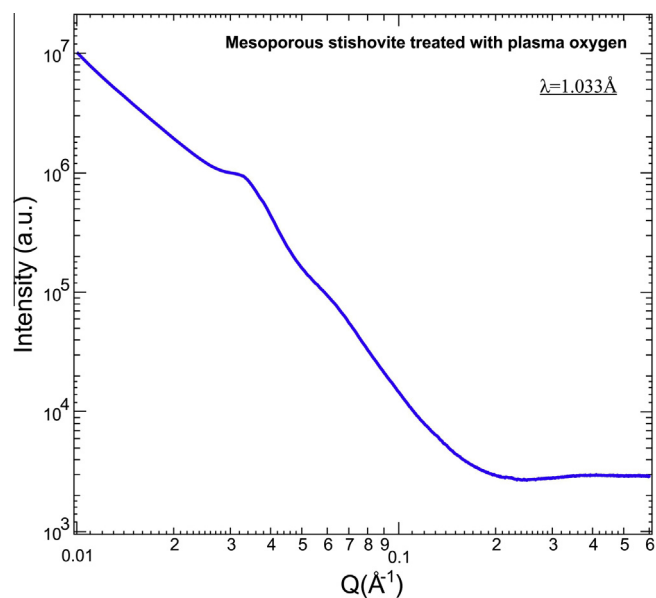


Fig. 4. SAXS pattern of stishovite recovered from 14 GPa and 500 °C after plasma etching treatment showing a weak periodicity.

in Fig. 5 where XRD patterns are representative of experiments quenched at temperatures between 100 and 500 °C. It can be seen

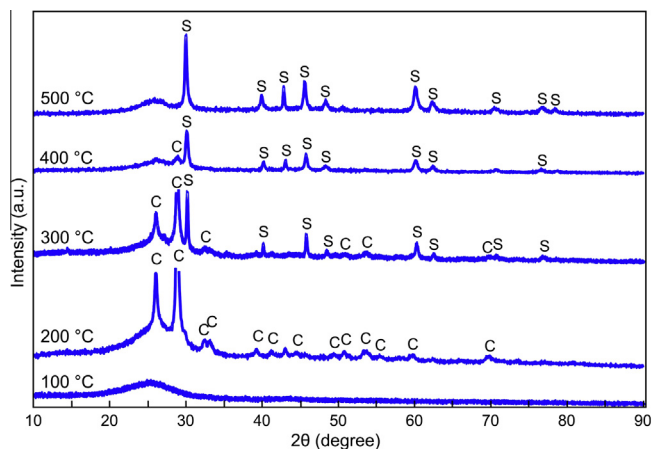


Fig. 5. XRD patterns (Cu K_{α} radiation) relative to experiments performed at 14 GPa and temperatures of 100–500 °C showing the evolution of the crystalline nature of the recovered samples from FDU-12/C composite. The lowest temperature of crystallization for stishovite (s) is shown to be about 500 °C, while metastable coesite (c) is obtained directly from the amorphous precursor at about 200 °C. No peaks representative of crystalline form of carbon are observed.

that at 100 °C no crystallization occurs. As the temperature is increased to 200 °C coesite starts to crystallize from the amorphous precursor. At a temperature of 300 °C the diffraction pattern shows evidence of the reduced intensity of peaks representative of coesite along with the appearance of new peaks that can be assigned to tetragonal stishovite. Peaks of coesite characterized by low intensity are still observed at 400 °C along with stishovite diffraction peaks. Finally, a diffraction pattern relative to the quenched sample from 14 GPa and 500 °C shows only reflections of stishovite. These results would confirm the crystallization of coesite well beyond its stability field [17,18] that, assuming absence of adsorbed moisture, can be likely explained by considering a kinetically controlled crystallization of metastable coesite as intermediate phase [19]. Our results provide evidence for mechanism of crystallization of stishovite from a FDU-12/carbon precursor at much lower temperature (~500 °C) than previous studies where temperatures ≥ 1000 °C are required [7,20], except when surface catalyzed or hydrous conditions are used [11,21]. The lowest temperature at which stishovite starts to form (~300 °C) likely corresponds to the minimum temperature at which the coesite–stishovite polymorphic transformation is energetically activated at a pressure of 14 GPa.

Time series experiments were also performed at 14 GPa and 500 °C in order to constrain the kinetics of crystallization at these P–T conditions. XRD data of the recovered samples demonstrate that stishovite formed after ~2 h, while a short run of about 1 h showed the presence of amorphous phase suggesting that no visible crystallization occurred from the silica precursor (Fig. S2). In addition, no crystallization of graphite from amorphous carbon is observed.

To understand the differences of the product material under the present P–T conditions with respect to previously synthesized materials, intermediate polymorphs were further analyzed. In particular, in one experiment synthetic coesite was quenched at 14 GPa and 200 °C, then calcined at 550 °C for 5 h. The crystalline nature was confirmed by XRD where the observed peaks could be assigned to monoclinic ($P2_1/a$, JCPDS file 14-0654) symmetry with refined lattice parameters of $a = 0.7196(5)$ nm, $b = 1.2364(7)$ nm, and $c = 0.71707(5)$ nm (Fig. S3). We observed the mesostructure by TEM (Fig. S4) but N_2 sorption measurements showed no significant N_2 uptake after oxygen plasma etching and calcination at 550 °C (see Supplemental informations). This appears in apparent contrast with results from a previous study [5]

where comparatively lower pressure was used than in our present study (12 vs. 14 GPa). This would suggest that increasing pressure of synthesis promotes pore-closure.

We also investigated the effects of amorphization of mesostructured stishovite. Stishovite recovered from 14 GPa and 500 °C was calcined at 450 °C in air for 5 h to remove carbon. The resulting powder was white in color suggesting the glassy nature also confirmed by the absence of peaks in the collected XRD patterns (Fig. S5). SEM image (Fig. S6) for this sample did not show the dotted texture previously observed, however, TEM images (Fig. S7a) showed a mesostructure with weak periodicity (Fig. S7b). The pore sizes and the pore wall thickness estimated by TEM were ~15 nm and ~5 nm, respectively. This would imply densification of the mesoporous pore wall structure during the amorphization of stishovite associated with the known transformation from the sixfold-coordinated to a fourfold-coordinated network [14,15] prior to complete oxidation of the carbon template.

SAXS measurements were also performed on mesostructured coesite and amorphous mesostructured silica glass after amorphization of stishovite and the results are shown in Fig. S8. An average pore size of 19 nm (within an uncertainty of about 5 Å) is clearly observed for both the samples with Q values around 0.033 \AA^{-1} , which corroborates the informations from TEM images and would exclude possible collapse of the pore structure. However, the broad bump has lower intensity than mesostructured coesite, which might imply further lowered periodicity.

4. Conclusion

Our results clearly show that mesostructured stishovite was obtained using the nanocasting route at pressure of 14 GPa at 500 °C starting from periodic mesostructured FDU-12/carbon composite precursor. At 14 GPa mesostructured coesite was also obtained at a temperature of 200 °C. Gas adsorption measurements on the recovered samples would suggest that the connectivity between the main mesopores might have been lost during the high-pressure synthesis, in contrast with previous studies where SBA-16/C composite was used as a precursor to form coesite but at lower pressure (12 GPa). SAXS measurements confirmed that the initial pore size of FDU-12/carbon is retained after crystallization of high density mesostructured stishovite being characterized by a pore size of 19 nm as also confirmed by TEM images. Potential applications of mesostructured stishovite would be in optical amplifications, laser systems, medical diagnostics or in electronics as low dielectric materials.

Acknowledgements

This work was supported as part of Energy Frontier Research in Extreme Environments Center (EFree), an Energy Frontier Research Center funded by the U.S. Department of Energy, Office of Science under Award Number DE-SC0001057. Dr. J. Wang is acknowledged for technical assistance using oxygen plasma etcher. SAXS experiment was performed in 12ID-B, Argonne National Laboratory, and Dr. Xiaobing Zuo is acknowledged for his technical support during the SAXS measurement. APS is supported by DOE-BES, under contract No. DE-AC02-06CH11357.

Appendix A. Supplementary data

Supplementary data associated with this article can be found, in the online version, at <http://dx.doi.org/10.1016/j.micromeso.2013.12.032>.

References

- [1] C.T. Kresge, M.E. Leonowicz, W.J. Roth, J.C. Vartuli, J.S. Beck, *Nature* 359 (1992) 710–712.
- [2] K. Na, C. Jo, J. Kim, K. Cho, J. Jung, Y. Seo, R.J. Messinger, B.F. Chmelka, R. Ryoo, *Science* 333 (2011) 328–332.
- [3] J. Jiang, J.L. Jorda, J. Yu, L.A. Baumes, E. Mugnaioli, M.J. Diaz-Cabanias, U. Kolb, A. Corma, *Science* 333 (2011) 1131–1134.
- [4] P. Mohanty, B. Kokoszka, C. Liu, M. Weinberger, M. Mandal, V. Stagno, Y. Fei, K. Landskron, *Microporous Mesoporous Mater.* 152 (2012) 214–218.
- [5] P. Mohanty, Y. Fei, K. Landskron, *J. Am. Chem. Soc.* 131 (2009) 9638–9639.
- [6] L. Sun, J. Yu, H. Zhang, Q. Meng, E. Ma, C. Peng, K. Yang, *Microporous Mesoporous Mater.* 98 (2007) 156–165.
- [7] N. Nishiyama, S. Seike, T. Hamaguchi, T. Irifune, M. Matsushita, M. Takahashi, H. Ohfuji, Y. Kono, *Scr. Mater.* 67 (2012) 955–958.
- [8] G. Wirmsberger, P. Yang, B.J. Scott, B.F. Chmelka, G.D. Stucky, *Spectrochim. Acta Part A* (2001). 2049–1060.
- [9] Anatoly N. Trukhin, Janis L. Jansons, Tatyana I. Dyuzheva, Ludmila M. Lityagina, Nikolai A. Bendeliani, *Solid State Commun.* 127(6), 2003, 415–418, doi: 10.1016/S0038-1098(03)00456-3.
- [10] N. Sahai, *J. Colloid, Interface Sci.* 252 (2002) 309–319.
- [11] P. Mohanty, D. Li, T. Liu, Y. Fei, K. Landskron, *J. Am. Chem. Soc.* 131 (2009) 2764–2765.
- [12] P. Mohanty, Y. Fei, K. Landskron, *High Pressure Res.* 29 (2009) 754–763.
- [13] C.M. Bertka, Y. Fei, *J. Geophys. Res.* 102 (1997) 5251–5264.
- [14] P.A. van Aken, T.G. Sharp, F. Seifert, *Phys. Chem. Miner.* 25 (1998) 83–93.
- [15] F. Dacheille, R.J. Zeto, R. Roy, *Science* 140 (1963) 991–993.
- [16] M. Grimsditch, S. Popova, V.V. Brazhkin, R.N. Voloshin, *Phys. Rev. B* 50 (1994) 12984–12986.
- [17] M. Akaogi, M. Oohata, H. Kojitani, H. Kawaji, *Am. Mineral.* 96 (2011) 1325–1330.
- [18] W. Yong, E. Dachs, A. Benisek, R.A. Secco, *Phys. Chem. Miner.* 39 (2012) 153–162.
- [19] A. Navrotsky, L. Mazeina, J. Majzlan, *Science* 319 (2008) 1635–1638.
- [20] J. Zhang, B. Li, W. Utsumi, R.C. Liebermann, *Phys. Chem. Miner.* 23 (1996) 1–10.
- [21] K. Spektor, J. Nysten, E. Stoyanov, A. Navrotsky, R.L. Hervig, *Proc. Natl. Acad. Sci. USA* 108 (2011) 20918–20922.